



LAWRENCE
LIVERMORE
NATIONAL
LABORATORY

Extending Regional Seismic Travel Time (RSTT) Tomography to New Regions

S. C. Myers, M. L. Begnaud, S. Ballard, W. S.
Phillips, M. E. Pasyanos

July 13, 2011

Monitoring Research Review
Tucson, AZ, United States
September 13, 2011 through September 15, 2011

Disclaimer

This document was prepared as an account of work sponsored by an agency of the United States government. Neither the United States government nor Lawrence Livermore National Security, LLC, nor any of their employees makes any warranty, expressed or implied, or assumes any legal liability or responsibility for the accuracy, completeness, or usefulness of any information, apparatus, product, or process disclosed, or represents that its use would not infringe privately owned rights. Reference herein to any specific commercial product, process, or service by trade name, trademark, manufacturer, or otherwise does not necessarily constitute or imply its endorsement, recommendation, or favoring by the United States government or Lawrence Livermore National Security, LLC. The views and opinions of authors expressed herein do not necessarily state or reflect those of the United States government or Lawrence Livermore National Security, LLC, and shall not be used for advertising or product endorsement purposes.

EXTENDING REGIONAL SEISMIC TRAVEL TIME (RSTT) TOMOGRAPHY TO NEW REGIONS

Stephen C. Myers¹, Michael L. Begnaud², Sanford Ballard³, W. Scott Phillips², Michael E. Pasyanos¹

¹Lawrence Livermore National Laboratory,

²Los Alamos National Laboratory,

³Sandia National Laboratory,

Sponsored by National Nuclear Security Administration

Contract No. DE-AC52-07NA27344¹, DE-AC04-94AL8500², DE-AC52-06NA25396³

ABSTRACT

Lowering the global seismic detection threshold can be accomplished by introducing data recorded at regional distances (<2000 km from the event) into global monitoring systems. Unfortunately, introduction of regional data degrades average epicenter accuracy compared to locations constrained solely by data recorded at greater distances. Location accuracy degrades because regional seismic travel time (RSTT) prediction error is generally greater than prediction error for waves that travel to greater distances. In previous work we developed a computationally efficient method to capture the 1st-order effects of 3-dimensional crust and upper mantle structure on RSTTs. Previous results demonstrate that RSTT prediction accuracy is greatly improved by seismic tomography, in which model velocities are adjusted so that predicted travel times are in agreement with travel times that are based on a data set of accurate event locations and arrival-time measurements. We have conducted RSTT tomography for the regional phases Pn, Pg, Sn, and Lg across Eurasia and for the Pn phase across North America. After tomography across Eurasia and North America, rigorous tests find that the standard deviation of Pn travel time residuals is reduced from approximately 1.75 seconds (ak135 model) to approximately 1.25 seconds. Further, the median location error is reduced from approximately 15 km to 9 km for network configurations that effectively average out measurement error.

Reduction of epicenter error, millisecond travel time computation, and the flexibility to compute travel times between arbitrary points on/in the globe all make the RSTT method ideal for routine location work and for use in seismic monitoring systems. Extension of RSTT tomography to additional regions is a necessary step towards making the RSTT approach universally attractive to monitoring agencies, such as the International Data Center at the Comprehensive Test Ban Treaty Organization (CTBTO), the National Earthquake Information Center (NEIC), and the International Seismic Centre (ISC). Geographic extension of RSTT tomography through regional cooperation is currently being pursued. In the regional cooperation approach, scientists from study regions participate in the development of high-quality data sets, tomography, and model validation. A regional cooperation approach works towards producing the most complete tomographic data set, and it provides a better understanding of the RSTT approach to the international scientific community.

OBJECTIVES

Previous reports on this project describe the development of a global model framework and computationally efficient method for predicting Regional Seismic Travel Times (RSTTs) (Myers et al., 2010a). In addition to the RSTT framework, tomographic studies are needed to tune velocity parameters in the RSTT Earth representation for optimal travel time prediction accuracy. To date, RSTT tomography has been conducted for regional phases Pn, Pg, Sn, and Lg across Eurasia, and for Pn across North America (Figure 1). Additional tomographic studies are needed in order to achieve accurate RSTT prediction everywhere possible.

We are pursuing the extension of RSTT tomography through international collaborative projects. The tasks for extending RSTT tomography to new areas are outlined, and an estimate of the improvement in location accuracy that may be achieved by using RSTT with a regional and a global monitoring network are presented.

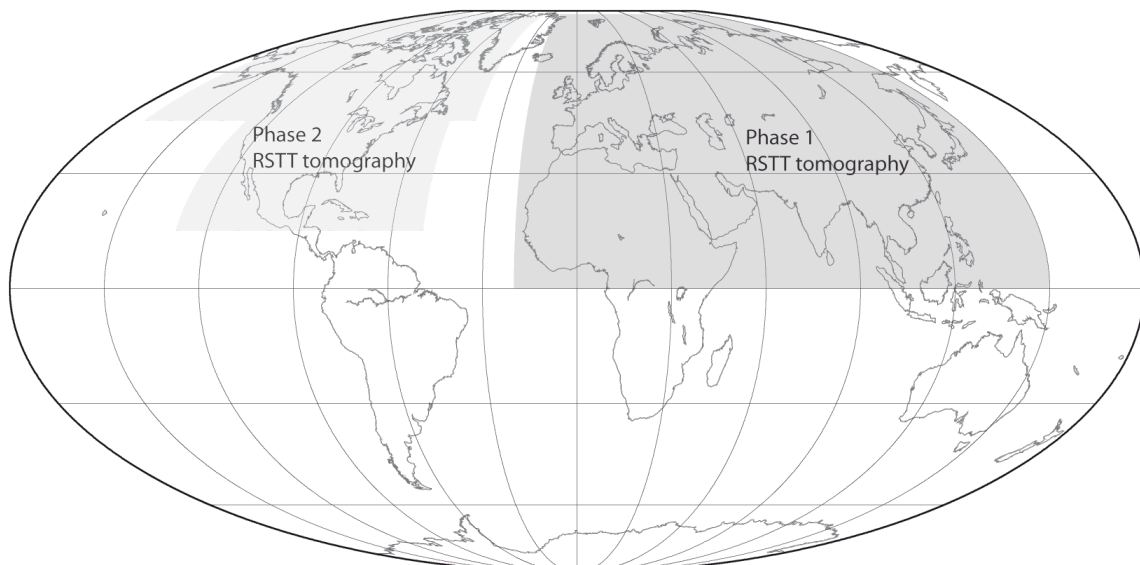


Figure 1. RSTT tomographic studies completed to date. Tomography for Pn, Pg, Sn, and Lg has been conducted across Eurasia (phase 1). North Africa was nominally included in Phase 1 tomography, but data coverage is poor. Tomography for Pn has been conducted across North America. Further tomographic studies are needed if RSTT is to provide universal improvement in regional travel time prediction.

RESEARCH ACCOMPLISHED

Previous Work

We have successfully developed an operations-ready method to capture the 1st-order effects of 3-dimensional crust and upper mantle structure on RSTTs (Myers et al., 2010a). Operations-ready, means that travel times must be computed in real-time from an arbitrary event location to an arbitrary station location without extending the time required to analyze the seismic data stream, including event location. After several years of code and model development, as well as rigorous testing, the RSTT travel time code and representation of crust and upper mantle seismic wave velocity has been provided to the U.S. National Data Center (NDC) and the National Earthquake Information Center (NEIC). The U.S. government is considering the release of the RSTT product to the International Data Center (IDC) – part of the Provisional Technical Secretariat (PTS) of the Comprehensive Nuclear Test Ban Organization (CTBTO), which would allow evaluation of the RSTT model and method by both U.S. and international monitoring agencies.

The NEIC utilizes an extensive regional network throughout North America. The improvement to travel time prediction and location accuracy for networks that are predominantly at regional distance, which we define as 100 km to 1500 km in this case, is well documented in Myers et al., (2010a) and Myers et al. (2010b) (Figures 2 and 3).

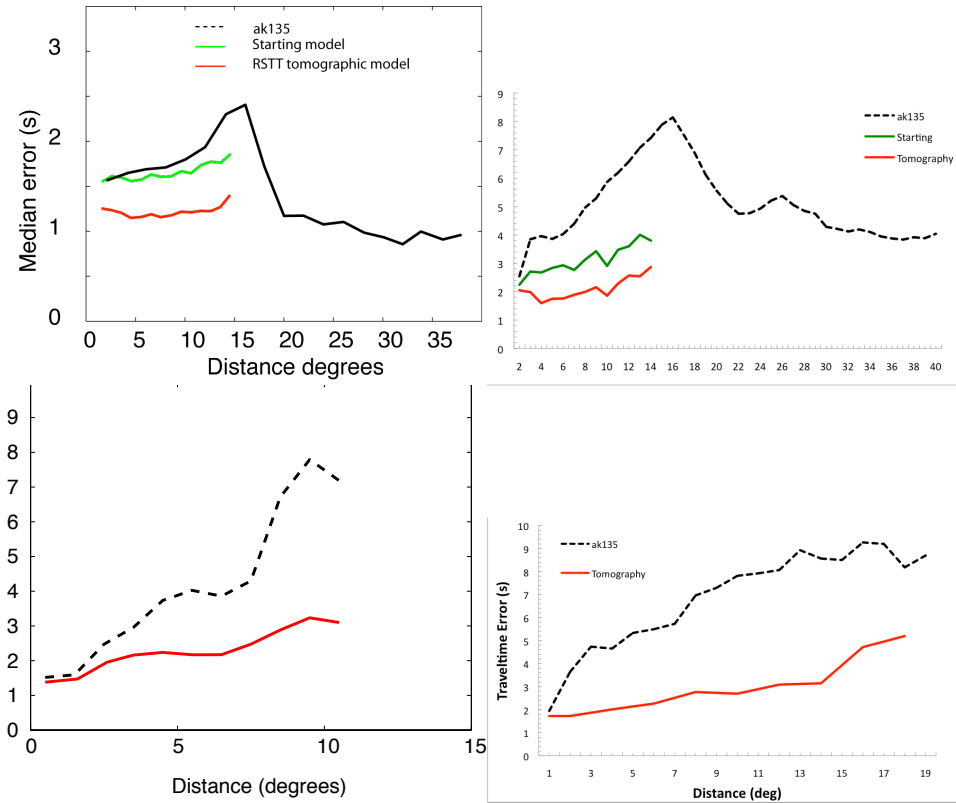


Figure 2. Travel time prediction error for Pn (upper left), Pg (lower left), Sn (upper right), and Lg (lower right) phases as a function of event-station distance in Eurasia. Black lines indicate ak135 predictions and red lines indicate RSTT tomography. Green line in the Pn plot is for model velocities based on a compilation of published and other work, which shows minimal improvement over ak135. Green line in the Sn plot is for model velocities

optimally scaled from the Pn tomography result, which shows that single-phase tomography is needed to achieve optimal travel time prediction.

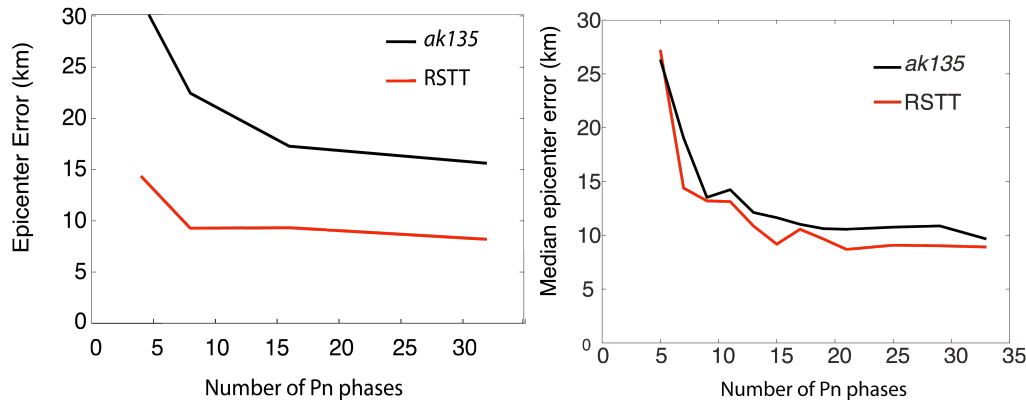


Figure 3. Median epicenter error vs. number of Pn phases. Eurasia (Right) and North America (Left). The large improvement in Eurasia is due to poor ak135 performance and meticulous data culling in the tomography and validation data sets. In North America ak135 performs better than in Eurasia and the degree of improvement using RSTT is reduced due to larger pick errors in the data set.

Regional picks are likely to be a smaller percentage of the overall data set for global monitoring networks like the IMS. Nonetheless, the greater probability of detection at regional distances is expected to result in regional picks being a significant percentage of the data set for small events. Figure 4 shows the degradation in location accuracy that is observed for a global set of events when 1 Pn phases is introduced to a P-wave (teleaseismic) data set. Figure 4 also shows the average number of phases used to locate events in the IDC's Reviewed Event Bulletin (REB) as a function of magnitude. For events below magnitude 4.0 the degradation in location is greater than ~5 km when 1 Pn phase is added, and when the magnitude is ~3.0 (5 P phases; off the graph) the average degradation in location is greater than 50 km.

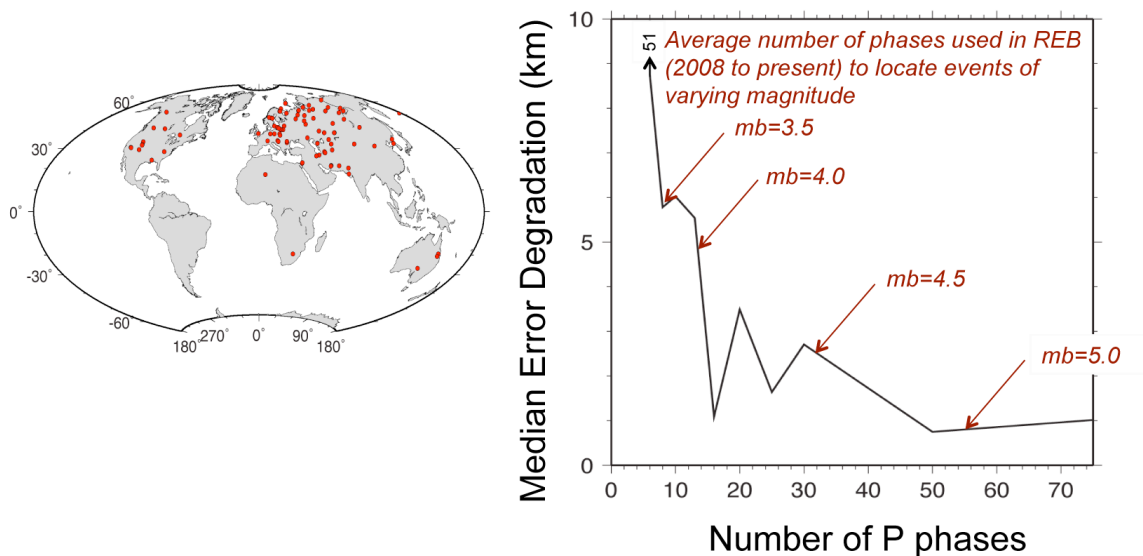


Figure 4. Degradation in epicenter accuracy when 1 Pn arrival time is introduced into a P-wave (teleseismic) arrival-time data set. Left, global set of events that was used for location tests. Most events are nuclear explosions with location accuracy of 1 km or better. Earthquakes with location accuracy of 5 km or better provide additional geographic coverage. Right, median degradation in epicenter accuracy vs. number of P arrivals (teleseismic) when 1 Pn arrival is introduced.

Model Parameterization

Myers et al. (2010a) provide a detailed description of RSTT model parameterization, travel time calculation, and tomographic formulation, and we provide a brief review here. Crust and upper mantle velocity structure are represented using radial velocity profiles at geographically distributed nodes (Figure 5). The nodes form a triangular tessellation that seamlessly covers the globe, and node spacing may be adjusted as needed. Nominal node spacing is approximately 1° for current RSTT models, and we have used 0.5° node spacing in North America, which is warranted by outstanding data coverage in the western U.S.. Velocity interfaces are defined by the radial distance from the center of the Earth, which allows us to explicitly build the GRS80 ellipsoid (Moritz, 1980) into the model and obviate travel time corrections for ellipticity (e.g Ballard et al., 2009).

We adopt the velocity versus depth profile in the crust from Pasyanos et al. (2004), which includes model layers for water, 3 types of sediments, upper crystalline crust, middle crust, and lower crust (Figure 5). The crustal layers overlay a mantle velocity profile that is simplified to two parameters: velocity at the Moho and a linear velocity gradient with depth. By interpolating model parameters from surrounding nodes – layer thickness, velocity, and mantle gradient – we generate a continuous model of the 3-D crust and laterally varying upper mantle.

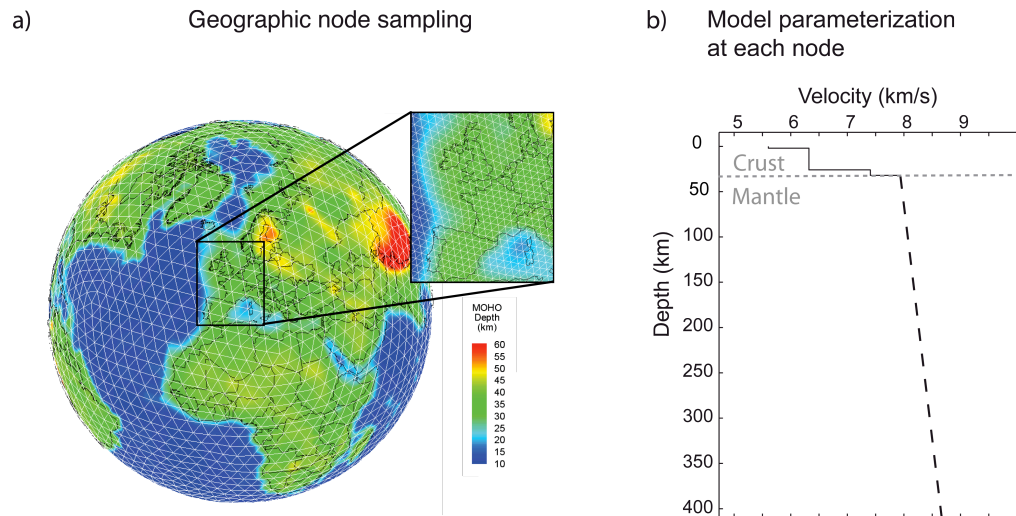


Figure 5. Global model parameterization. a) An example tessellation with approximately 5° grid spacing. The inset shows our nominal 1° node spacing. Color indicates Moho depth of the starting model. b) An example velocity/depth profile as defined at each node. The mantle portion of the profile is specified by the velocity at the crust/mantle interface and a linear gradient. (Reproduced from Myers et al., 2010)

Travel Time Calculation

Parameterization of upper mantle velocity with a linear gradient facilitates an approximation for Pn travel time that enables real-time computation (~1 millisecond). Computation of Pn travel time at near-regional distance (<700 km) commonly assumes that the Pn phase propagates as a head wave, with a ray-path that follows the contour of the Moho (e.g. Hearn, 1984). The head wave assumption results in poor travel time prediction at far-regional distance (>~700 km) because the Pn ray can dive appreciably into the mantle due to a positive velocity gradient with depth and Earth sphericity (e.g. Zhao and Xie, 1993; Ritzwoller et al., 2003; Hearn et al., 2004). To more accurately predict Pn at far-regional distances, Zhao (1993) and Zhao and Xie (1993) employ a constant linear velocity gradient in the upper mantle for the whole study area.

The Zhao (1993) and Zhao and Xie (1993) travel time calculation is similar to the widely used approach of Hearn (1984), with an additional term (γ) introduced to account for diving rays. The travel-time calculation is

$$TT = \sum_{i=1}^N d_i s_i + \alpha + \beta + \gamma \quad (1)$$

where d and s are the distance and slowness (taken as 1/velocity below the Moho) in each of the i segments comprising the great-circle path between Moho pierce points near the event and station, α and β are the crustal travel times at the source and receiver, and γ (described below).

From Zhao (1993) and Zhao and Xie (1993),

$$\gamma = \frac{c^2 X_m^3}{24 V_0} \quad (2)$$

where X_m is the horizontal distance traveled in the mantle, and V_0 is a regional average of mantle velocity at the Moho. $c = g * s + 1/r$, where $1/r$ is an Earth flattening correction and r is the radius at which a ray enters and exits the linear velocity gradient, g (Helmberger, 1973; Zhao and Xie, 1993). This approximation is valid when $ch \ll 1$, where h is the bottoming depth of the ray in a linear velocity gradient.

We use a spatially varying mantle velocity gradient, c (Phillips et al., 2007), and we calculate γ by averaging c along the ray track. V_0 remains an average Pn velocity over the whole model, which allows us to take advantage of linear tomographic inversion methods (see below). Tests find that using a global average for V_0 introduces negligible travel-time error when Pn velocities range from 7.5 km/s to 8.3 km/s.

Coding Details

The RSTT computer code written in C++, with easy to use interfaces to C, FORTRAN, and java languages. RSTT has been compiled on Sun, Linux, and Windows operating systems. Porting to other operating systems is possible.

Tasks For Extending RSTT Tomography

RSTT model refinement has 5 essential components.

- 1) A prior model is built that includes lateral variability of the geologic layers that comprise the crust.
- 2) A high quality data set of event locations and arrival-time observations is compiled for use in tomography and for model validation.
- 3) Tomographic inversion is used to adjust model velocities so that travel time predictions are in agreement with the high-quality data set.
- 4) Assessment of travel time error is accomplished by comparing model predictions to the validation data set (not used in tomography).
- 5) Event location accuracy is assessed and location uncertainty estimates are validated.

Task 1: The current RSTT model includes laterally variable geologic layers that are based on an LLNL/LANL effort to compile the results of geophysical studies across Eurasia (Pasyanos et al., 2004; Steck et al., 2004); layer depth are derived from CRUST2.0 (Bassin et al., 2000) elsewhere. Crustal layers are not modified during the RSTT tomographic inversion, and large errors in layer depths – particularly the crust-mantle boundary (Moho) – will result in travel time errors that cannot be fully corrected by tomography. Therefore, an effort to adjust crustal boundaries in the RSTT model should be made. After compilation of the geological information is completed, node-specified adjustments to model layers can be easily made using the RSTT code.

Task 2: The national laboratories have an ongoing effort to collect and reconcile seismic bulletins that comprise the vast majority of available events and arrival time measurements. International collaborators can provide unique data sets that may not be openly available. Collaborators may also measure arrival times for signals that have not been previously measured. The new data sources ensure improved geographic data coverage and tomographic resolution. The additional measurements can be reconciled with existing databases at the national laboratories. Quality control for arrival time measurements is achieved based on the procedures outlined in Flanagan et al. (2008). For RSTT phases, the maximum event-station distance range is set to 15° . Beyond 15° the Pn and Sn phases may interact with velocity discontinuities at ~ 410 km and ~ 660 km depth, and RSTT travel time predictions become inaccurate due to deviations from the RSTT linear-velocity gradient. The minimum event-station distance range for Pn and Sn is determined by the post-critical refraction for a wave interacting with the Moho. There is no physical reason to limit the distance range for either Pg or Lg, but we remove all measurement beyond 15° both because picks errors become large for these phases at great distances and for consistency with Pn and Sn. All picks are evaluated against an uncertainty budget that accounts for event mislocation, a global average of *ak135* prediction uncertainty, and arrival-time measurement uncertainty (See Myers et al., 2010a); residuals outside the 95th interquartile are removed.

Evaluation of epicenter accuracy (e.g. Bondár et al., 2004) after relocation with the superset of arrival times results in a database of events with well-characterized uncertainty. Contribution of location constraints based on non-seismic information (e.g. known mine) is extremely valuable.

Because the goal of this work is to predict RSTTs for real-time monitoring, it is important that RSTT error is unbiased relative to travel time predictions at greater distance. Previous efforts have achieved unbiased Pn error by using an *ad hoc* travel time correction (Yang et al., 2004). To achieve unbiased RSTT error, we recomputed each event origin time using at least 10 P-wave arrivals. A regional model that is known to produce unbiased residuals with respect to teleseismic error may also be used to estimate origin time. The hypocenter is then fixed during the tomographic procedure, which forces Pn prediction error to be unbiased relative to teleseismic P-wave error.

Task 3: The Pn travel time (Equation 1) lends itself to a linear tomographic formulation. Because our primary objective is to improve travel-time prediction, we avoid the use of parameters that would not be part of a subsequent travel-time calculation (e.g. event and station time terms). In matrix form, the tomographic system of equations is:

$$\begin{bmatrix} x_1^1 & \dots & x_N^1 & -\frac{x_1^1(X_m)^3}{24V_oX_m} & \dots & -\frac{x_N^1(X_m)^3}{24V_oX_m} & \sum_{p=1}^Q \frac{l_{1p}^1}{v_{1p}} & \dots & \sum_{p=1}^Q \frac{l_{Np}^1}{v_{Np}} \\ \vdots & & & & \ddots & & & & \vdots \\ x_1^K & \dots & x_N^K & -\frac{x_1^K(X_m)^3}{24V_oX_m} & \dots & -\frac{x_N^K(X_m)^3}{24V_oX_m} & \sum_{p=1}^Q \frac{l_{1p}^K}{v_{1p}} & \dots & \sum_{p=1}^Q \frac{l_{Np}^K}{v_{Np}} \end{bmatrix} \begin{bmatrix} s_1 \\ \vdots \\ s_N \\ c_1^2 \\ \vdots \\ c_N^2 \\ a_1 \\ \vdots \\ a_N \end{bmatrix} = \begin{bmatrix} t^1 \\ \vdots \\ t^K \end{bmatrix} \quad (3)$$

Regularization

where

- t = travel time
- s = mantle slowness below the Moho (a.k.a. Pn slowness)
- x = Pn distance (or weight) for each model node
- c = normalized velocity gradient, $v=v_o(1+cz)$
- X_m = length of Pn ray path in the mantle
- V_o = average Pn velocity
- v = velocity of a crustal layer
- k = index on K paths (travel-time observations)
- p = index on Q crustal layers
- l = length of the ray path in a specified crustal layer (determined by layer thickness and ray parameter in Equations (2) and (3)).
- a = node-specific adjustment to the slowness of each crustal layer (crustal modifier).

The tomographic equation solves for the model slowness below the Moho, s (a.k.a. Pn slowness), the square of mantle velocity gradient, c^2 , and a scalar adjustment to crustal slowness, a . We initially solve for a model with overly smooth velocity and gradient variations to improve the starting model and test for outlier data. To find optimal smoothing during tomography, we test a range of parameters, looking for an appropriate trade-off between smoothing and reduction in travel time residuals. Once optimal smoothing is determined, a full inversion is performed.

Task 4: Non-circular assessment of travel time error is determined using data that are set aside from the tomographic inversion. Typically, 10% of the data are used for validation tests and measures are taken to ensure that the validation data set provides even geographic sampling. Simple residuals (observed travel time minus predicted travel time) are the fundamental quantity that is used to measure travel time improvement. First-order assessment of residuals commonly reveals a strong trend with event-station distance. Therefore, residuals are binned by distance and trends are defined by averages or interquartiles of residuals in each bin. Measurement error is estimated based on the spread of residuals observed at a single station for events that comprise a cluster (i.e. the path to the station is nearly the same, so the prediction error should be highly correlated). A large set of station-cluster estimates is used to establish distance-dependant measurement errors. The distance-dependant variance of the pick error is subtracted from the residual error to estimate the variance of RSTT prediction error.

Task 5: Improvement in hypocenter (latitude, longitude, depth, and time) accuracy begins with relocating events for which locations are known or for which hypocenter uncertainty is well characterized and small. The distance between estimated and known hypocenter, accounting for any uncertainty, forms the fundamental metrics for hypocenter improvement. The lateral position of the event (epicenter) is the most commonly measured component of hypocenter accuracy, followed by depth and origin time. Epicenter is the most common metric for several reasons: epicenter has considerable utility in monitoring, epicenter is typically better constrained than other hypocenter parameters, and for most regional and teleseismic data sets there is an inherent trade off between estimates of depth and origin time that results in poor resolution for both parameters (i.e. the model cannot help resolve the trade off). Hypocenter error is evaluated as a function of the number of arrival time data, the types of phases or combination of phases, and the configuration of the network (azimuthal and distance coverage).

Validation of location uncertainty estimates is based on the percentage times that known locations occur inside computed coverage regions (i.e. error ellipse for an epicenter). The percentage of occurrences of the known location inside of the error ellipse is then compared to the confidence level of the ellipse (e.g. Myers and Schultz, 2000), while accounting for any uncertainty in the location of the validation event (e.g. Bondar and McLaughlin, 2009). Because the location coverage region is derived from estimates of residual variance (see Evernden, 1969), validation of location error estimates is a check that errors have been adequately estimated. If the number of occurrences agrees with the confidence level, within expected fluctuations, then the uncertainties are validated and estimated location uncertainties may be used to infer location accuracy.

CONCLUSIONS AND RECOMMENDATIONS

We have developed an operations-ready method to improve the accuracy of regional seismic travel time (RSTT) prediction. The method includes an Earth representation with a 3-dimensional crust, a laterally variable mantle velocity at the crust-mantle boundary, and a linear velocity gradient with depth in the mantle. The travel time method exploits an analytical approximation for travel time in a linear velocity gradient, which enables computation of travel time through the model in approximately 1 millisecond with a common desktop computer. Improved travel time prediction accuracy is reliably achieved only after seismic tomography is used to tune model velocities so that predicted travel times agree with travel times for a high-quality data set. To date, RSTT tomography has been conducted for regional phases Pn, Pg, Sn, and Lg across Eurasia, and for Pn across North America (Figure 1). Additional tomographic studies are needed in order to achieve accurate RSTT prediction everywhere possible. Collaboration with the international community is the best path forward for extending RSTT tomography to new regions. We specify 5 tasks for extending RSTT tomography to new regions. The tasks entail data collection, improving the Earth model, and testing.

ACKNOWLEDGEMENTS

Funding for this project is provided by the Ground-Based Nuclear Detonation Detection program (Leslie Casey program manager) within NNSA/NA22. We also thank our colleagues and collaborators at AFTAC, who worked closely with us at the formative stages of the RSTT project.

REFERENCES

- Ballard, S., J. R. Hipp, and C. J. Young (2009), Efficient and accurate calculation of ray theory seismic travel time through variable resolution 3D Earth models, *Seismol. Res. Lett.*, **80**, 989 - 999.
- Bassin, C., G. Laske, and G. Masters (2000), The current limits of resolution for surface wave tomography in North America, *EOS Trans AGU*, 81, F897.
- Bondár, I., S.C. Myers, E.R. Engdahl, E.A. Bergman, Epicenter accuracy based on seismic network criteria, *Geophys. Jour. Int.*, **156**, 483–496, 2004.
- Bondár, I., S.C. Myers, E.R. Engdahl, E.A. Bergman, Epicenter accuracy based on seismic network criteria, *Geophys. Jour. Int.*, **156**, 483–496, 2004.
- Bondár, I., K.L. McLaughlin. A New Ground Truth Data Set For Seismic Studies, Seismological Research Letters Volume 80, Number 3, May/June 2009.
- Evernden, J. F. (1969). Precision of epicenters obtained by small numbers of world wide stations, *Bull. Seism. Soc. Am.*, **59**, 1365-1398.
- Flanagan, M.P., D.A. Dodge, and S.C. Myers (2008). GT merge Process: Version 2.0, LLNL Technical Report, LLNL-TR-410856.
- Hearn, T. M. (1984). Pn travel times in southern California, *Jour. Geophys. Res.*, **89**, 1843-1855.
- Hearn, T.M., S. Wang, J.F. Ni, Z. Xu, Y. Yu, and X. Zhang (2004). Uppermost mantle velocities beneath China and surrounding regions, *J. Geophys. Res.*, **109**, B11301, doi:10.1029/2003JB002874.
- Helmberger, D.V. (1973). Numerical seismograms of long-period body waves from seventeen to forty degrees, *Bull. Seismol. Soc. Am.*, 63, 633-646, 1973.
- Kennett, B.J.N., E.R. Engdahl and R. Buland (1995). Constraints on seismic velocities in the Earth from traveltimes, *Geophys. J. Int*, **122**, 108-124.
- Moritz, H. (1980). Geodetic reference system 1980. *Bull. Geodesique. Paris*, **54** (3).
- Myers, S.C., C.A. Schultz, Improving sparse-network location with Bayesian kriging and teleseismically constrained calibration events, *Bull. Seismol. Soc. Am.*, **90**, 199-211, 2000.
- Myers, S.C., M. L. Begnaud, S. Ballard, M. E. Pasyanos, W. S. Phillips, A. L. Ramirez, M. S. Antolik, K. D. Hutchenson, J. Dwyer, and C. A. Rowe, and G. S. Wagner (2010a). A crust and upper mantle model of Eurasia and North Africa for Pn travel time calculation, *Bull. Seismol. Soc. Am.*, **100**, 640-656.
- Myers, S.C., M. L. Begnaud, S. Ballard, A. L. Ramirez, W.S. Phillips, M. E. Pasyanos, H. Benz, and R. P. Buland (2010b). A regional seismic travel time model for North America, *2010 Monitoring Research Review: Ground-Based Nuclear Explosion Monitoring Technologies*, Orlando Fl., <https://na22.nnsa.doe.gov/prod/researchreview/2010/PAPERS/03-08.PDF>.
- Pasyanos, M.E., W.R. Walter, M.P. Flanagan, P. Goldstein, and J. Bhattacharyya (2004). Building and testing an a priori geophysical model for western Eurasia and North Africa, *Pure. And Applied Geophys.*, **161**, 235-281.
- Phillips, W.S., M.L. Begnaud, C.A. Rowe, L.K. Steck, S.C. Myers, M.E. Pasyanos, and S. Ballard (2007). Accounting for lateral variations of the upper mantle gradient in Pn tomography studies, *Geophys. Res. Lett.*, **34**, doi:10.1029/2007GL029338, 2007.
- Ritzwoller, M. H., N. M. Shapiro, A. Levshin, E. A. Bergman, and E. R. Engdahl (2003). The ability of a global 3-D model to locate regional events, *J. Geophys. Res.* **108**, 2353, doi 10.1029/2002JB002167.
- Steck, L. K., C. A. Rowe, M. L. Begnaud, W. S. Phillips, V. L. Gee, and A. A. Velasco (2004), Advancing seismic event location through difference constraints and three-dimensional models, *paper presented at 26th Seismic Research Review - Trends in Nuclear Explosion Monitoring*, Orlando, Florida.
- Yang, X., I. Bondár, J. Bhattacharyya, M. Ritzwoller, N. Shapiro, M. Antolik, G. Ekström, H. Israelsson, and K. McLaughlin (2004). Validation of Regional and Teleseismic Travel-Time Models by Relocating Ground-Truth Events, *Bull. Seism. Soc. Amer.*, **94**, 897–919.
- Zhao, L.-S. (1993). Lateral variations and azimuthal isotropy of Pn velocities beneath Basin and Range province, *Jour. Geophys. Res.*, **98**, 22,109-22,122.
- Zhao, L.-S., and J. Xie (1993). Lateral variations in compressional velocities beneath the Tibetan Plateau from Pn travelttime tomography, *Geophys. J. Int.*, **115**, 1070-1084.